

See discussions, stats, and author profiles for this publication at: <https://www.researchgate.net/publication/231231393>

Interaction of Copper(II) with Ditopic Pyridyl- β -diketone Ligands: Dimeric, Framework, and Metallogel Structures

ARTICLE in CRYSTAL GROWTH & DESIGN · MARCH 2011

Impact Factor: 4.89 · DOI: 10.1021/cg101629w

CITATIONS

11

READS

80

11 AUTHORS, INCLUDING:



[Jack Clegg](#)

University of Queensland

163 PUBLICATIONS 2,203 CITATIONS

[SEE PROFILE](#)



[Christopher R K Glasson](#)

James Cook University

25 PUBLICATIONS 581 CITATIONS

[SEE PROFILE](#)



[Katrina Anne Jolliffe](#)

University of Sydney

155 PUBLICATIONS 2,592 CITATIONS

[SEE PROFILE](#)



[Leonard F Lindoy](#)

University of Sydney

388 PUBLICATIONS 6,484 CITATIONS

[SEE PROFILE](#)

Interaction of Copper(II) with Ditopic Pyridyl- β -diketone Ligands: Dimeric, Framework, and Metallogel Structures

Melanie Dudek,[†] Jack K. Clegg,[‡] Christopher R. K. Glasson,[§] Norman Kelly,[†] Kerstin Gloe,[†] Karsten Gloe,^{*†} Alexandra Kelling,^{||} Hans-Jürgen Buschmann,[†] Katrina A. Jolliffe,[‡] Leonard F. Lindoy,^{*‡} and George V. Meehan[§]

[†]Department of Chemistry and Food Chemistry, TU Dresden, 01062 Dresden, Germany

[‡]School of Chemistry, University of Sydney, NSW 2006, Australia

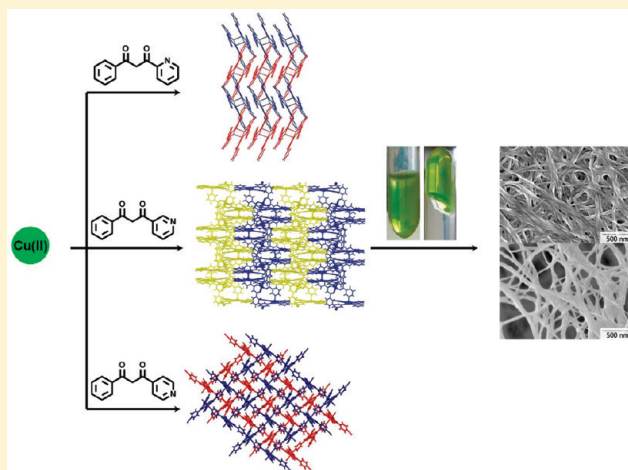
[§]School of Pharmacy and Molecular Sciences, James Cook University, Townsville 4811 Queensland, Australia

^{||}Institute of Chemistry, University of Potsdam, 14469 Potsdam, Germany

[†]German Textile Research Centre DTNW, 47798 Krefeld, Germany

Supporting Information

ABSTRACT: The interaction of Cu(II) with three β -diketone ligands of type $R^1C(O)CH_2C(O)R^2$ (where $R^1 = 2$, 3-, or 4-pyridyl and $R^2 = C_6H_5$, respectively), HL^1 – HL^3 , along with the X-ray structures and the pK_a values of each ligand, are reported. HL^1 yields a dimeric complex of type $[Cu(L^1)_2]_2$. In this structure, two deprotonated HL^1 ligands coordinate in a *trans* planar fashion around each Cu(II) center, one oxygen from each CuL_2 unit bridges to an axial site of the second complex unit such that both Cu(II) centers attain equivalent five-coordinate square pyramidal geometries. The two-substituted pyridyl groups in this complex do not coordinate, perhaps reflecting steric factors associated with the closeness of the pyridyl nitrogen to the attached (conjugated) β -diketonato backbone of each ligand. The remaining two Cu(II) species, derived from HL^2 and HL^3 , are both coordination polymers of type $[Cu(L)_2]_n$ in which the terminal pyridine group of each ligand is intermolecularly linked to an adjacent copper center to generate the respective infinite structures. HL^2 was also demonstrated to form a fibrous metallogel when reacted with $CuCl_2$ in an acetonitrile/water mixture under defined conditions.



■ INTRODUCTION

The synthesis of new metal coordination polymers, including new metal organic frameworks, has been given increasing attention over recent years, in part motivated by their ready preparation via self-assembly processes and by the prospect of generating new materials exhibiting useful and/or unusual properties.^{1–11} Thus, systems showing luminescent,^{12–14} nonlinear optical,¹⁵ catalytic,¹⁶ magnetic spin-crossover,^{17,18} as well as other less common magnetic properties¹⁹ have all been documented. Linear difunctional ligand systems (such as, for example, 4,4'-bipyridyl or terephthalic acid) have very commonly been employed to connect metal units in the formation of such materials, while nonlinear bifunctional ligands have received somewhat less attention. Nevertheless, both categories have now been demonstrated to form a range of diverse metallo-polymeric structures. For example, both linear and nonlinear, pyridyl-substituted β -diketonato ligands have been successfully employed for the

generation of a range of interesting coordination polymers. In these hetero difunctional ligand systems, the β -diketone fragment has the pyridyl substituent attached either to the “central” carbon atom (that is, the carbon between the two keto functions) or in a terminal position with respect to this fragment. Thus, the linear bifunctional derivative, 3-(4-pyridyl)pentane-2,4-dione, has been demonstrated to be an effective ligand for generating a number of one- (1D) and two-dimensional (2D) coordination polymers incorporating a range of metal ions;^{20–24} linear polymeric, ladder, and square-grid architectures have all been observed. A corresponding nonlinear ligand in which the pyridyl group is coupled to a β -diketonato fragment via a “bent” thioether linkage has also been demonstrated to yield porous 2D and three-

Received: December 8, 2010

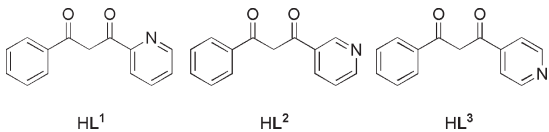
Revised: February 9, 2011

Published: March 10, 2011

dimensional (3D) networks with Cu(II) and Zn(II).²⁵ In other studies, a number of pyridyl terminally substituted difunctional β -diketone derivatives have also been used to form both homo- and heteronuclear coordination polymers.^{20,26,27} It is clear that both of the above categories of ligand, each of which contains "classical" pyridyl and β -diketonato metal binding motifs, are extremely versatile systems for generation of metal coordination polymers displaying diverse architectures. These interesting structural arrangements have, in part, provided a motivation for undertaking the present investigation.

Finally, it is noted that pyridine has been shown to react with Cu(II) β -diketonates to form corresponding pyridine adducts,²⁸ and a related two step synthetic procedure involving Cu(II) complexes of dibenzoyl- or benzoylacetyl methane and a bifunctional heterocyclic amine ligand has been employed to produce a range of corresponding metallo-frameworks.^{29–31}

We now report the results of a structural study of the three isomeric ligands HL¹–HL³ and their complexes with Cu(II). While these diketo derivatives were first reported almost 60 years ago³² and some preliminary results on their Cu(II) complexation were discussed in the 1960s,³³ since then only two reports have been published on metal complexation by such systems [describing structural details of mixed valent Mn(II)/Mn(III) tetra- and hexanuclear manganese cluster complexes with HL¹ that show interesting magnetic properties];^{34,35} a recent further publication has appeared relating to the antimicrobial activity of uncomplexed HL¹ and HL².³⁶



■ EXPERIMENTAL SECTION

Materials and Methods. All reagents and solvents were purchased from commercial sources and used without purification with the exception of tetrahydrofuran (THF), which was dried over sodium wire before use. NMR spectra were recorded on a Bruker DRX500 spectrometer, and HRMS were determined using a Bruker ESQUIRE mass spectrometer. Elemental analyses were performed on a vario Micro Cube analyzer.

General Preparation of HL¹–HL³. These were prepared by a modification of the procedure reported by Levine and Snead.³¹ The required methylester and acetophenone (see below) in dry THF were added to a suspension of sodium amide in dry THF at room temperature. The reaction mixture was refluxed for 6 h over which time the mixture turned brown. The reaction was quenched with acetic acid and water (40 mL), and the organic (THF) and aqueous phases were separated. The aqueous phase was washed three times with diethylether (40 mL), and the organic phases were combined and dried over anhydrous sodium sulfate. The solvent was removed under reduced pressure to yield the crude product, which was purified by column chromatography employing silica gel. Yields and characterization details for each product are given below.

1-Phenyl-3-(2-pyridyl)-1,3-propandione (HL¹). This was prepared as a yellow solid from sodium amide (0.895 g, 23 mmol), methyl picolinate (1.238 g, 10 mmol), and acetophenone (2.41 g, 20 mmol) in THF (42 mL). Yield, 1.56 g (6.94 mmol, 69%). Found: C, 74.41; H, 5.44; N, 5.91. Calcd for C₁₄H₁₁NO₂: C, 74.65; H, 4.92; N, 6.22%. ¹H NMR δ (500 MHz CDCl₃): 16.42 (br s, enol, 1H), 8.84 (d, aromatic, 1H), 8.33 (d, aromatic, 1H), 8.21 (d, aromatic, 2H), 8.15 (t, aromatic,

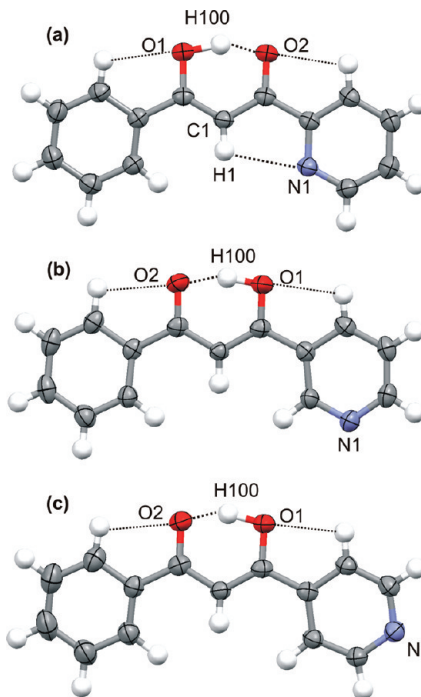


Figure 1. X-ray structures of (a) HL¹, (b) HL², and (c) HL³ showing the intramolecular hydrogen bonds.

1H), 7.98 (br s, –CH= enol, 1H), 7.69 (t, aromatic, 1H), 7.59 (t, aromatic, 1H), 7.52 ppm (t, aromatic, 1H). ESI-MS: *m/z* 226.0 (M + H)⁺.

1-Phenyl-3-(3-pyridyl)-1,3-propandione (HL²). This was prepared as a pale yellow solid from sodium amide (0.79 g, 20 mmol), methyl nicotinate (1.401 g, 10 mmol), and acetophenone (2.568 g, 21 mmol) in THF (42 mL). Yield, 1.72 g (7.66 mmol, 77%). ¹H NMR δ (300 MHz CDCl₃): 16.71 (br s, enol, 1H), 9.20 (br s, aromatic, 1H), 8.78 (d, aromatic, 1H), 8.27 (dd, aromatic, 1H), 8.01 (d, aromatic, 2H), 7.59 (t, aromatic, 1H), 7.52 (t, aromatic, 2H), 7.45 (t, aromatic, 1H), 6.87 ppm (s, –CH= enol, 1H). ESI-MS: *m/z* 226.0 (M + H)⁺.

1-Phenyl-3-(4-pyridyl)-1,3-propandione (HL³). This was prepared as a pale yellow solid from sodium amide (0.49 g, 12 mmol), methyl isonicotinate (0.622 g, 5 mmol), and acetophenone (1.358 g, 11 mmol) in 25 mL of THF. Yield, 0.826 g (3.667 mmol, 73%). ¹H NMR δ (500 MHz CDCl₃): 16.34 (br s, enol, 1H), 8.92 (br d, aromatic, 2H), 8.37 (d, aromatic, 2H), 8.04 (d, aromatic, 2H), 7.67 (t, aromatic, 1H), 7.55 (t, aromatic, 2H), 7.03 ppm (s, –CH= enol, 1H). ESI-MS: *m/z* 226.0 (M + H)⁺.

Complex Synthesis. Synthesis of [Cu(L¹)₂]_n·HL¹ (50 mg, 0.22 mmol) in dry THF (10 mL) was added to Na₂CO₃ (0.5 g, ~5 mmol) suspended in dry THF (15 mL). The mixture was stirred for 1 h before Cu(NO₃)₂·3H₂O (26.58 mg, 0.11 mmol) in THF (15 mL) was added dropwise, and the mixture was stirred at 35 °C for 2 h. Diffusion of a diethylether–hexane mixture (1/1, v/v) into the green solution yielded green needles after a few days. Found: C, 65.84; H, 4.48; N, 4.93%. Calcd for C₂₈H₂₀CuN₂O₄: C, 65.68; H, 3.94; N, 5.47%. ESI-MS: *m/z* 512.1 [Cu(L¹)₂ + H]⁺.

Synthesis of [Cu(L²)₂]_n·HL² (100.3 mg, 0.45 mmol) in dry THF (10 mL) was added to Na₂CO₃ (0.51 g, ~5 mmol) suspended in dry THF (5 mL). This mixture was stirred for 1 h before CuCl₂·2H₂O (38.8 mg, 0.23 mmol) in THF (15 mL) was added dropwise, and stirring was continued at room temperature for 2 h. Slow evaporation of a small amount of this solution over 24 h yielded a green crystalline product, which was isolated and washed with THF. Found: C, 66.05; H, 4.05; N, 5.58%. Calcd for C₂₈H₂₀CuN₂O₄: C, 65.68; H, 3.94; N, 5.47%. ESI-MS: *m/z* 512.1 [Cu(L²)₂ + H]⁺.

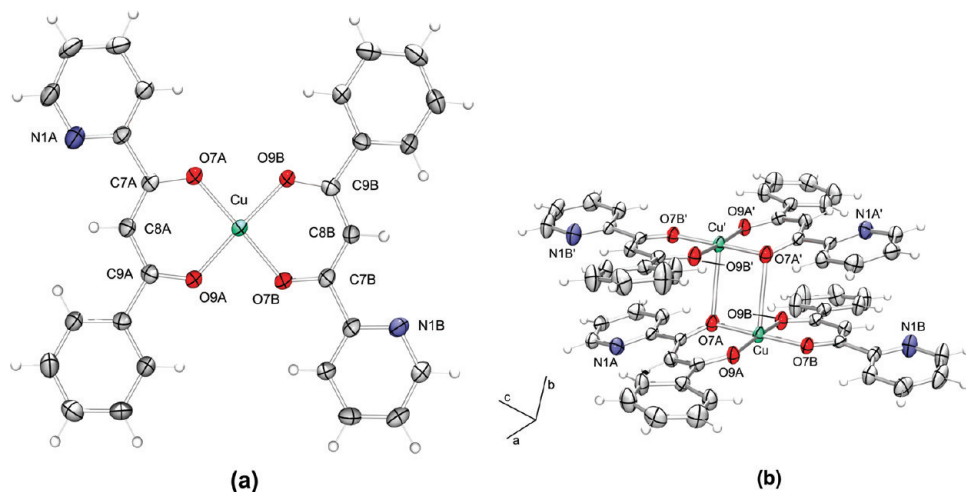


Figure 2. (a) ORTEP representation of the asymmetric unit of $[\text{Cu}(\text{L}^1)_2]_2$. (b) ORTEP representation of the dinuclear dimer of $[\text{Cu}(\text{L}^1)_2]_2$, shown with 50% probability ellipsoids.

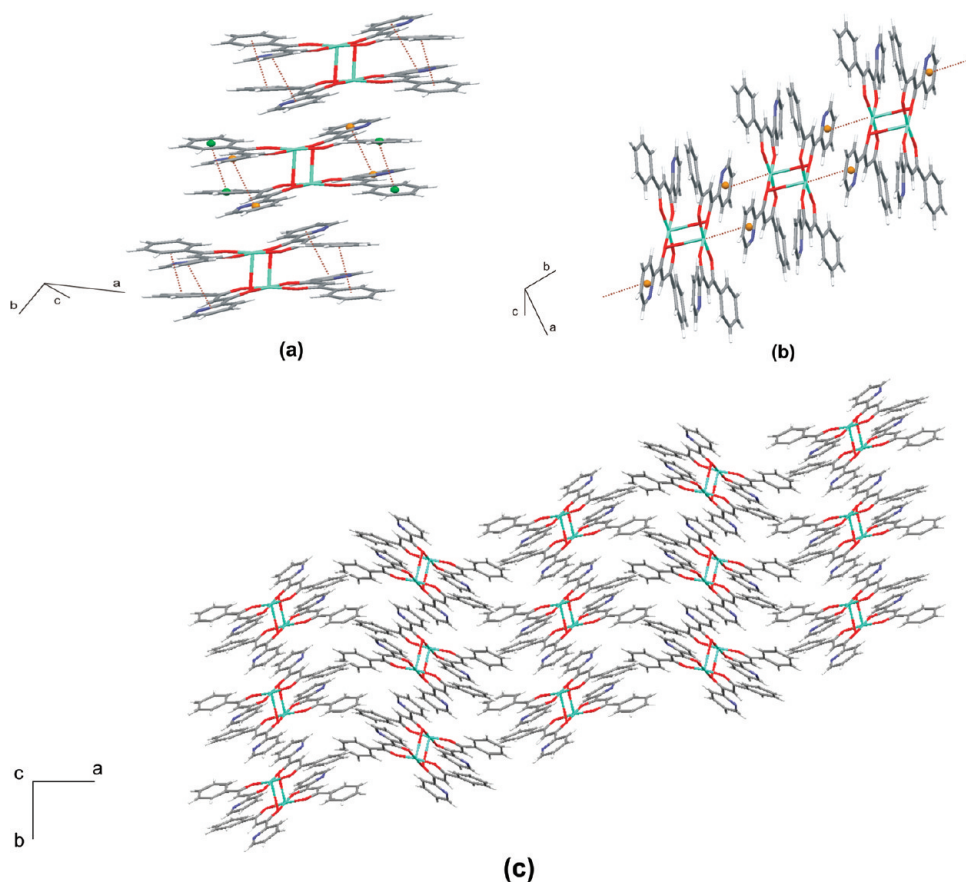


Figure 3. (a) $\pi-\pi$ interactions within the $[\text{Cu}(\text{L}^1)_2]_2$ dimers and (b) Cu(II)- π interactions between the dimer units and (c) the 3D structure of $[\text{Cu}(\text{L}^1)_2]_2$.

Synthesis of $[\text{Cu}(\text{L}^3)_2]_n \cdot \text{HL}^3$ (50 mg, 0.22 mmol) in dry THF (5 mL) was added to Na_2CO_3 (0.5 g, ~5 mmol) suspended in THF (15 mL). This mixture was stirred for 1 h before $\text{Cu}(\text{NO}_3)_2 \cdot 3\text{H}_2\text{O}$ (26.6 mg, 0.11 mmol) in THF (15 mL) was added dropwise. The solution was warmed to 35 °C, and stirring was continued for 2 h. Diffusion of a diethylether-hexane-mixture (1/1, v/v) into the green solution yielded green cuboidal crystals after several days. Found: C, 65.86; H, 4.29; N, 5.29%. Calcd for $\text{C}_{28}\text{H}_{20}\text{CuN}_2\text{O}_4$: C, 65.68; H, 3.94; N, 5.47%. ESI-MS: m/z 512.1 [$[\text{Cu}(\text{L}^3)_2 + \text{H}]^+$].

Metallogel Preparation and Characterization. For investigating metallogel formation, solutions of ligand HL^2 (0.2 mmol, 45.05 mg) and $\text{CuCl}_2 \cdot 2\text{H}_2\text{O}$ (0.2 mmol, 34.11 mg) in 20 mL of an acetonitrile/water mixture (v/v 1:1) were prepared and mixed in varying mole fractions (x) between x (ligand) = 0.1 and 0.9. Gelation was

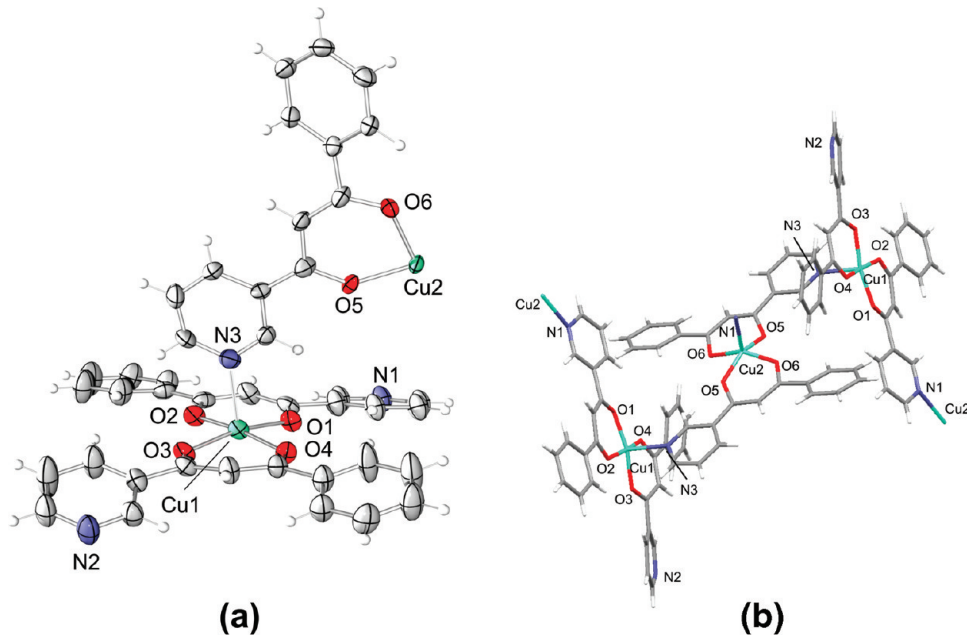


Figure 4. (a) ORTEP representation of the asymmetric unit of $\text{Cu}(1)(\text{L}^2)_2$, shown with 50% probability ellipsoids, and (b) the connection between individual chelate units. N1 coordinates to Cu2, and N2 remains uncoordinated.

obtained immediately in the samples for mole fractions between x (ligand) = 0.2–0.6. SEM analyses were undertaken on xerogel samples with an average thickness of 4–6 mm formed by evaporation of the gel to dryness under vacuum at 120° for 6 h. Sample preparation involved placing a dry amount of gel on carbon-coated grids and sputtering with a Au/Pd alloy. Cryogel samples were obtained by freezing the gel samples at -20°. The overlaying solvent was removed, and the samples were evaporated to dryness at -10° and 0.370 mbar overnight using a freeze dryer. Sample preparation involved placing a dried amount of gel on grids, coating with silver lacquer, and then sputtering with a Au/Pd alloy. Images were obtained using a DSM 982 Gemini (Zeiss) and accelerating voltage of 3 and 5 kV.

■ RESULTS AND DISCUSSION

Ligand X-ray Structures and pK_a Values. The X-ray structures of HL^1 – HL^3 are illustrated in Figure 1a–c. As is normal for such systems, in each case, the β -diketone fragment is in its enol form. Interestingly, the enolic proton is attached to O1, the oxygen adjacent to the terminal aryl ring in the case of HL^1 , but in HL^2 and HL^3 , it is adjacent to the 3- or 4-pyridyl group, probably reflecting the near electronic equivalence of these two aromatic ring types in relation to the attached β -diketone fragment. All three structures reveal the presence of the expected strong resonance-assisted intramolecular hydrogen bond³⁷ involving O1–H \cdots O2. For example, the O1–H100 \cdots O2 distance in HL^1 is 1.398 Å, and the angle is 157.7°. Weaker intramolecular C–H \cdots O1 (O2) and C–H \cdots N hydrogen bonds³⁸ together with weak intermolecular hydrogen bonds and π – π interactions are also evident in each case, leading to 3D packing arrangements in the crystal structures of these ligands (see the Supporting Information).

The pK_a values of the β -diketone ligands were determined potentiometrically in an ethanol/water mixture (2:1 v/v) and show the expected weak acidic character of the ligands. The values increase in the order HL^3 (7.66 ± 0.02) < HL^2 (8.16 ± 0.05) < HL^1 (8.40 ± 0.01), with the values for HL^1 and HL^2 being slightly higher than the corresponding constants in water.³⁹

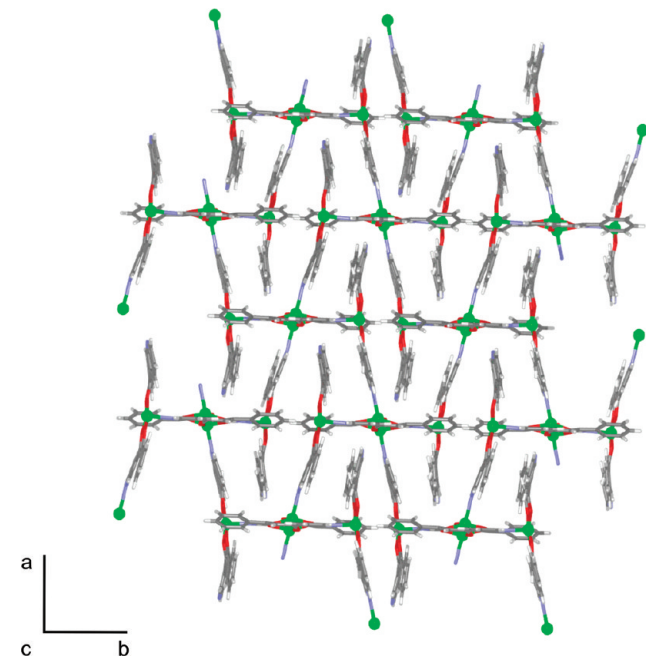


Figure 5. Schematic representation of a part of one of the lattice layers present in $[\text{Cu}(\text{L}^2)_2]_n$. Both disordered positions of Cu2 are shown.

X-ray Structures of Cu(II) Complexes. Dimeric $[\text{Cu}(\text{L}^1)_2]_2$ and polymeric $[\text{Cu}(\text{L}^2)_2]_n$ and $[\text{Cu}(\text{L}^3)_2]_n$ complexes were formed by reaction of $\text{Cu}(\text{NO}_3)_2 \cdot 3\text{H}_2\text{O}$ or $\text{CuCl}_2 \cdot 2\text{H}_2\text{O}$ with 2 equiv of the respective ligands in THF in the presence of a stirred suspension of sodium carbonate as base. Green crystals suitable for X-ray analysis were obtained by slow diffusion or direct crystallization from the reaction solution. In the case of HL^2 , an identical complex could be also isolated from an acetonitrile–water mixture without addition of base.

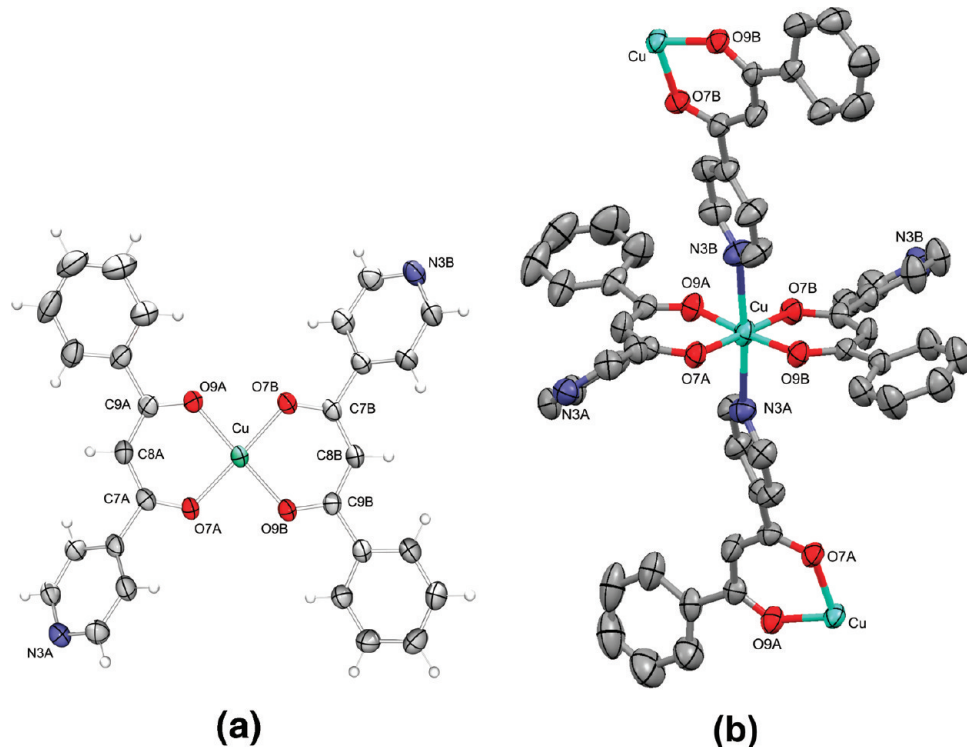


Figure 6. (a) ORTEP representation of the asymmetric unit of $[\text{Cu}(\text{L}^3)_2]_n$, and (b) ORTEP representation of the connection of alternate copper centers, shown with 50% probability ellipsoids.

The structure of $[\text{Cu}(\text{L}^1)_2]_2$ (Figure 2a) shows that two deprotonated HL^1 ligands coordinate in a *trans* planar fashion around each central copper ion, with all four $\text{Cu}-\text{O}$ distances being essentially equal at 1.91–1.92 Å. The structure (Figure 2b) is a dinuclear dimer in which one oxygen from each monomeric complex unit bridges to an axial site of the second complex unit and vice versa such that each metal center in the dimer attains an equivalent five-coordinate square pyramidal geometry ($\tau = 0.09$).⁴⁰ The $\text{Cu}-\text{Cu}$ distance in each dimer is 3.3 Å, and the axial (bridging) $\text{Cu}-\text{O}$ bonds (namely, $\text{Cu}-\text{O}7\text{A}'$ and $\text{Cu}'-\text{O}7\text{A}$) are Jahn–Teller elongated at 2.69 Å, with the $\text{O}7\text{A}-\text{Cu}-\text{O}7\text{A}'$ angle being 89.3°.

The terminal 2-pyridyl groups of each coordinated ligand are not bound, perhaps reflecting steric factors associated with the closeness of the 2-pyridyl nitrogen donor to the remainder of the ligand backbone. Individual pyridyl groups and phenyl rings lie opposite each other within each dimer unit (Figure 3a). The centroid–centroid distances are 4.03 and 4.11 Å, suggesting that marginal $\pi-\pi$ interactions may be present between opposing rings. The offset arrangement between successive dimeric units is shown in Figure 3b. Each Cu(II) center is located 3.6 Å from the centroid of a pyridyl ring present in an adjacent dimer unit, in accordance with the presence of weak “axial” interactions between the copper centers and the π -systems of these rings.^{41–48} When viewed from off the *c*-crystallographic axis the zigzag pattern formed by adjacent columns is illustrated in Figure 3c. No other significant intermolecular interactions are present between dimer units.

A variable temperature magnetic investigation of $[\text{Cu}(\text{L}^1)_2]_2$ has been undertaken. No magnetic exchange between the copper centers in the dimer units was observed, undoubtedly reflecting the extended distance (3.3 Å) between these centers and the elongated Jahn–Teller distortion present in the $\text{O}7\text{A}-\text{Cu}$ bridges (2.69 Å).

The structure of $[\text{Cu}(\text{L}^2)_2]$ shows the presence of two nonequivalent copper centers, $\text{Cu}1$ and $\text{Cu}2$, with the latter being disordered over two positions (across an inversion center) with 50% occupancy in each case (Figure 4). Each of the copper centers is five-coordinated, with four oxygen donors occupying the basal plane and a pyridyl donor occupying the apical position resulting in square-pyramidal coordination geometry. Interestingly, the N2-containing pyridyl ring is not involved in the Cu(II) coordination but participates in the formation of an additional weak hydrogen bond to the phenyl ring of the neighboring layer ($\text{CH}\cdots\text{N}2 = 2.65$ Å), strengthening the network arrangement.

The structure forms an infinite 2D lattice. If $\text{Cu}1(\text{L}^2)_2$ is considered a two-connecting node and the $\text{Cu}2(\text{L}^2)_2$ fragment is considered a four-connecting node, then, overall, the structure can be described effectively as a distorted (4,4)-network⁴⁹ (Figure 5).

Because of the disorder present in the $\text{Cu}2$ site, however, there are a large number of randomly distributed disruptions in the lattice structure (that is, ~50% of the $\text{Cu}2-\text{N}3$ bonds illustrated in Figure 6 are absent). Adjacent layers pack closely together with a number of $\pi-\pi$ interactions (showing both face-to-face and edge-to-face orientations) being present between the layers.

The molecular structure of $[\text{Cu}(\text{L}^3)_2]_n$ is shown in Figure 6a. In analogy with the structures discussed above, the two deprotonated HL^3 ligands adopt a *trans* planar arrangement around one copper ion with $\text{Cu}-\text{O}$ distances of ~1.95 Å.

At alternate copper centers, the structure is extended in a second direction at approximately right angles to generate a layer arrangement (Figure 6b), incorporating slightly rhomboidal cavities (angles: $\text{O}7\text{A}-\text{Cu}-\text{N}3\text{A}$, 95.0°; $\text{O}7\text{B}-\text{Cu}-\text{N}3\text{B}$, 98.3°; $\text{O}7\text{A}-\text{Cu}-\text{N}3\text{B}$, 82.5°; and $\text{O}7\text{A}-\text{Cu}-\text{N}3\text{A}$, 95.0°) with the copper ions defining the corners of each rhombus (Figure 7).

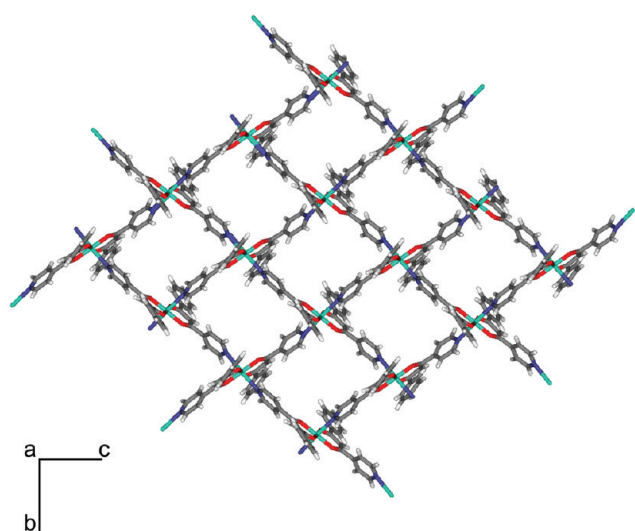


Figure 7. 2D lattice structure of $[\text{Cu}(\text{L}^3)_2]_n$, showing the rhomboidal cavities.

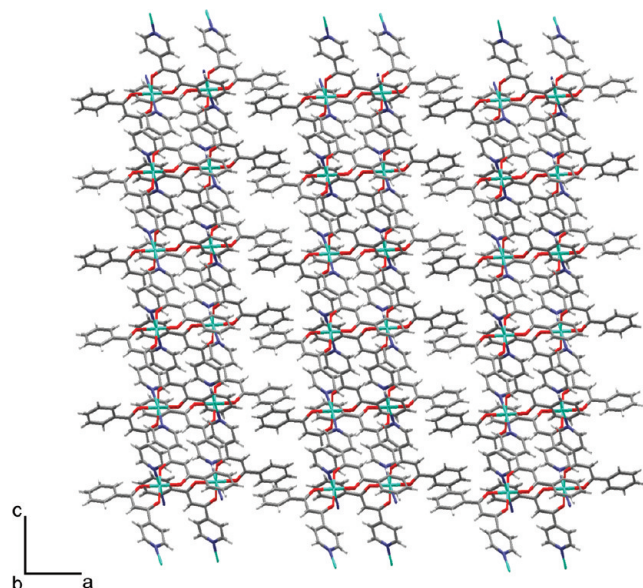


Figure 8. Layer pairs in $[\text{Cu}(\text{L}^3)_2]_n$ showing how the phenyl groups occupy the intervening space between them.

Phenyl rings from an adjacent layer occupy the above rhomboidal cavities such that the layers are paired, and a discontinuity is present between successive layer pairs (Figure 8). No strong intermolecular interactions are present between the layer pairs; however, the second phenyl group from each complex unit points outward from these pairs, occupying the intervening space between them.

The results of a related study by Domasevitch et al.²⁷ are of direct relevance to the present system. These workers reported the structure of the Cu(II) complex of 1-(4-pyridyl)butan-1,3-dione, the analogue of HL^3 in which a methyl group replaces the terminal phenyl ring. In this case, a related gridlike structure was generated in which each rhomboidal cavity is occupied by a methyl group from a neighboring complex unit; within this system, the second methyl from each complex unit is directed

into the space between successive layer pairs. Reflecting the smaller size of the terminal methyl groups (relative to the phenyl groups in HL^3), solvent methanol molecules also occupy this space in this case.

Metallogel Formation with HL^2 . While studying the complexation properties of HL^2 toward Cu(II), metallogel formation was observed in an acetonitrile–water mixture (v/v 1:1) for mole fractions (x) of HL^2 between 0.2 and 0.6 in the presence of CuCl_2 (Figure 9). HL^2 was not observed to form a gel by itself under a range of experimental conditions; also, the use of $\text{Cu}(\text{NO}_3)_2$ or $\text{Cu}(\text{CH}_3\text{COO})_2$ as copper salts does not lead to metallogel formation. Gelation was easily initiated by mixing the respective solutions without the addition of a separate base. Obviously, the pyridine substituent of HL^2 promotes the proton abstraction in this case. The product gels are stable at room temperature, but their formation can be reversed by shaking.

Over recent years, metallogels based on various ligand types have attracted increasing interest due to their potential for use in a number of application options.^{50–55} To the best of our knowledge, the present system is the first example of a low molecular weight gelator based on a metal-coordinated simple β -diketone skeleton. In this context, we are only aware of gel formation by the Cu(II) β -diketonate of dibenzoyl methane substituted by eight $\text{C}_9\text{H}_{19}\text{O}$ functions⁵⁶ and an alkyl chain-appended bis- β -diketone compound incorporating a diaminocyclohexane platform. This later gel can be strengthened by the addition of Co(II), Ni(II), or Cu(II).⁵⁷

The above copper-containing gel was investigated by scanning electron microscopy (SEM). SEM micrographs of the dried (xerogel) and freeze-dried (cryogel) gel obtained for HL^2 at the mole fraction $x = 0.5$ alongside the packing motif in the corresponding single crystal of the polymeric complex $[\text{Cu}(\text{L}^2)_2]_n$ are shown in Figure 10. The gel is characterized by a typical fibrous network, with the fibers having diameters of up to 40 nm. Such an arrangement is assumed to be mainly based on the interplay of multiple weak interactions in the system. In this context, analysis of the solid state structure appears to give some preliminary insights into the observed gel formation, especially in view of the fact that only HL^2 gives gels (the two isomeric ligands HL^1 and HL^3 did not form gels under comparable conditions to that used for HL^2). As shown in Figure 4, the single crystal structure of the polymeric $[\text{Cu}(\text{L}^2)_2]_n$ is characterized by typical square planar coordination of the two β -diketonato units for the Cu(II) center in a similar manner to the other two complexes. However, in the case of $[\text{Cu}(\text{L}^2)_2]_n$, additional weak hydrogen bonds of the uncoordinated pyridine nitrogen and multiple π – π interactions of the aromatic fragments are present that lead to packed extended columnar arrays. The observed diverse weak binding pattern differs markedly from that in the two other complexes and is manifested by very different solid state structures. By analogy, the difference in the weak interaction possibilities between the above three complexes very likely plays an important role in the gelation process. Weak interactions involving the gelator and solvent molecules have been well established to be a decisive parameter in gel formation.

It is interesting to note that HL^1 and HL^3 did not form metallogels under comparable conditions to that used for HL^2 . It is likely that this difference in the ligand series can be attributed to the changing position (from 2- and 4-position to 3-position) of the pyridine nitrogen atom in the pyridyl substituents, leading to different structural arrangements and, in particular, differences in the weak intermolecular interactions linking complex units. This

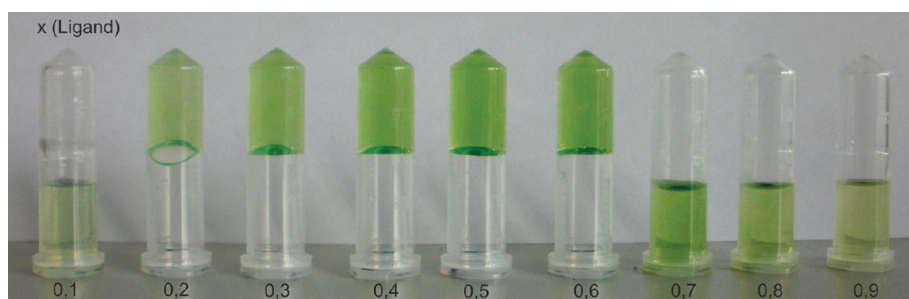


Figure 9. Vials containing an acetonitrile/water (v/v 1:1) solution of HL^2 and increasing amounts of $\text{CuCl}_2 \cdot 2\text{H}_2\text{O}$ showing metallogel formation at mole fractions (x) of HL^2 between 0.2 and 0.6 after mixing.

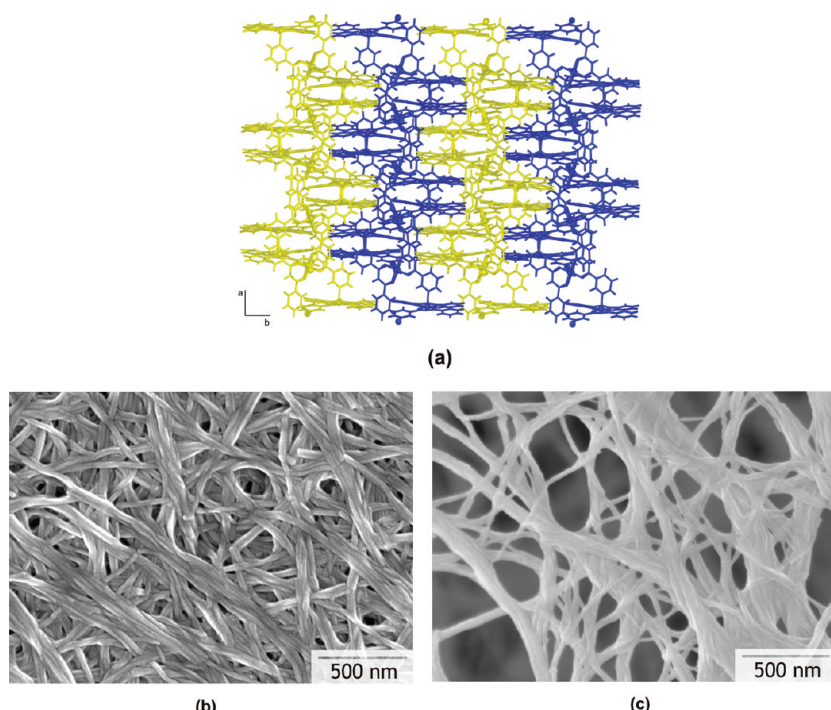


Figure 10. Comparison of the “columnar” structure of $[\text{Cu}(\text{L}^2)_2]_n$ found in the crystal packing (a) and fibrous structure in the xerogel (b) and in the cryogel (c). The latter representations are SEM micrographs of the metallogel after drying and freeze drying in vacuum at the mole fraction $x = 0.5$.

conclusion is supported by significant differences in the solid state Cu(II) complex structures of the diketonates. As shown by their X-ray structures, in comparison to $[\text{CuL}^1]^2$ and $[\text{Cu}(\text{L}^3)]_n$, the new gelator $[\text{Cu}(\text{L}^2)_2]_n$ shows additional hydrogen bonds and $\pi-\pi$ stacking interactions, which may contribute to stabilization of the columnar structure in this case.

■ CONCLUSION

In the present study, we have synthesized and characterized new examples of a dimeric and two polymeric metal β -diketonato complex structures whose interesting molecular architectures clearly reflect the presence (and availability) of additional pyridyl functionality present on each of the β -diketone derivatives of type HL^1-HL^3 . Whereas the chelating binding pattern in all three complexes is comparable, there are significant differences in the intermolecular interactions that are present between the complex units. Along this ligand series, only HL^2 was demonstrated to form a metallogel with CuCl_2 underscoring the role of the different pyridyl substituents in controlling the hydrogen bonding and $\pi-\pi$

interaction patterns occurring between the respective complexes. More generally, the study also illustrates that solid state structural data can be a useful adjunct to the investigation of metallogelation behavior of the type discussed above.

■ ASSOCIATED CONTENT

S Supporting Information. X-ray crystallographic details of the ligand and Cu(II) complex structures including H-bond and π -interaction data, selected bond lengths and angles, IR, ^1H NMR and UV-vis spectroscopic data, additional figures of the structures and information about the gel formation. The data is also deposited in the Cambridge Crystallographic Data Centre (CCDC), deposition numbers CCDC 814650-814652 ($\text{HL}1-\text{HL}3$) and CCDC 814653-814655 $\{[\text{Cu}(\text{L}1)_2]_2, [\text{Cu}(\text{L}2)_2]_n, [\text{Cu}(\text{L}3)_2]_n\}$. These data can be obtained free of charge via www.ccdc.cam.ac.uk/data_request/cif, or by emailing data_request@ccdc.cam.ac.uk, or by contacting The Cambridge Crystallographic Data Centre, 12, Union Road,

Cambridge CB2 1EZ, UK; fax: +44 1223 336033. This material is available free of charge via the Internet at <http://pubs.acs.org>.

AUTHOR INFORMATION

Corresponding Author

*E-mail: (K.G.) karsten.gloe@chemie.tu-dresden.de or (L.F.L.) lindoy@chem.usyd.edu.au.

ACKNOWLEDGMENT

We thank the Deutsche Forschungsgemeinschaft, the Australian Research Council, and the IPDF Scheme (University of Sydney) for support. M.D. acknowledges gratefully the Deutsche Bundesstiftung Umwelt for a Ph.D. grant. We also thank Berthold Kersting and Jochen Lach, University Leipzig, for magnetic measurements.

REFERENCES

- (1) Thomas, K. M. *Dalton Trans.* **2009**, 1487.
- (2) Perry, J. J.; Kravtsov, V. C.; McManus, G. J.; Zaworotko, M. J. *J. Am. Chem. Soc.* **2007**, 129, 705.
- (3) McManus, G. J.; Wang, Z.; Beauchamp, D. A.; Zaworotko, M. J. *Chem. Commun.* **2007**, 5212.
- (4) Kepert, C. J. *Chem. Commun.* **2006**, 695.
- (5) Antonioli, B.; Bray, D. J.; Gloe, K.; Gloe, K.; Heßke, H.; Lindoy, L. F. *CrystEngComm* **2006**, 8, 748.
- (6) Lee, E. Y.; Jang, S. Y.; Suh, M. P. *J. Am. Chem. Soc.* **2005**, 127, 6374.
- (7) Fujimoto, K.; Perry, J. J.; McManus, G. J.; Zaworotko, M. J. *Chem. Commun.* **2004**, 2534.
- (8) Batten, S. R.; Murray, K. S. *Coord. Chem. Rev.* **2003**, 246, 103.
- (9) Carlucci, L.; Ciani, G.; Proserpio, D. M. *Coord. Chem. Rev.* **2003**, 246, 247.
- (10) Armstrong, R. S.; Atkinson, I. M.; Carter, E.; Mahinay, M. S.; Skelton, B. W.; Turner, P.; Wei, G.; White, A. H.; Lindoy, L. F. *Proc. Nat. Acad. Sci.* **2002**, 99, 4987.
- (11) Masaoka, S.; Furukawa, S.; Chang, H.-C.; Mizutani, T.; Kitagawa, S. *Angew. Chem., Int. Ed.* **2001**, 40, 3817.
- (12) Allendorf, M. D.; Bauer, C. A.; Bhakta, R. K.; Houk, R. J. T. *Chem. Soc. Rev.* **2009**, 38, 1330.
- (13) Wen, L.; Lu, Z.; Lin, J.; Tian, Z.; Zhu, H.; Meng, Q. *Cryst. Growth Des.* **2007**, 7, 93.
- (14) Ma, L.; Evans, O. R.; Foxman, B. M.; Lin, W. *Inorg. Chem.* **1999**, 38, 5837.
- (15) Zhang, L.-J.; Yu, J.-H.; Xu, J.-Q.; Lu, J.; Bie, H.-Y.; Zhang, X. *Inorg. Chem. Commun.* **2005**, 8, 638.
- (16) Lee, J.-Y.; Farha, O. K.; Roberts, J.; Scheidt, K. A.; Nguyen, S.-B. T.; Hupp, J. T. *Chem. Soc. Rev.* **2009**, 38, 1450.
- (17) Kurmoo, M. *Chem. Soc. Rev.* **2009**, 38, 1353.
- (18) Halder, G. J.; Kepert, C. J.; Moubaraki, B.; Murray, K. S.; Cashion, J. D. *Science* **2002**, 298, 1762.
- (19) Maspoch, D.; Ruiz-Molina, D.; Veciana, J. *J. Mater. Chem.* **2004**, 14, 2713.
- (20) Vreshch, V. D.; Lysenko, A. B.; Chernega, A. N.; Sieler, J.; Domasevitch, K. V. *Polyhedron* **2005**, 24, 917.
- (21) Vreshch, V. D.; Lysenko, A. B.; Chernega, A. N.; Howard, A. K.; Krautscheid, H.; Sieler, J.; Domasevitch, K. V. *Dalton Trans.* **2004**, 2899.
- (22) Chen, B.; Fronczek, F. R.; Maverick, A. W. *Inorg. Chem.* **2004**, 43, 8209.
- (23) Chen, B.; Fronczek, F. R.; Maverick, A. W. *Chem. Commun.* **2003**, 2166.
- (24) Vreshch, V. D.; Chernega, A. N.; Howard, J. A. K.; Sieler, J.; Domasevitch, K. V. *Dalton Trans.* **2003**, 1707.
- (25) Won, T.-J.; Clegg, J. K.; Lindoy, L. F.; McMurry, J. C. *Cryst. Growth Des.* **2007**, 7, 972.
- (26) Faniran, J. A.; Patel, K. S.; Nelson, L. O. *J. Inorg. Nucl. Chem.* **1976**, 38, 77.
- (27) Domasevitch, K. V.; Vreshch, V. D.; Lysenko, A. B.; Krautscheid, H. *Acta Crystallogr.* **2006**, C62, m443.
- (28) Lennartson, A.; Hakansson, M.; Jagner, S. *New J. Chem.* **2007**, 31, 344.
- (29) Dey, S. K.; Bag, B.; Zhou, Z.; Chan, A. S. C.; Mitra, S. *Inorg. Chim. Acta* **2004**, 357, 1991.
- (30) Li, B.; Lang, J.; Wang, S.; Zhang, Y. *J. Chem. Crystallogr.* **2005**, 35, 547.
- (31) Soldatov, D. V. *J. Chem. Crystallogr.* **2006**, 36, 747.
- (32) Levine, R.; Snead, J. K. *J. Am. Chem. Soc.* **1951**, 73, 5614.
- (33) Wolf, L.; Hennig, H. Z. *Anorg. Allg. Chem.* **1964**, 329, 301.
- (34) Yang, C.; Wernsdorfer, W.; Tsai, Y.-J.; Chung, G.; Kuo, T.-S.; Lee, G.-H.; Shieh, M.; Tsai, H.-L. *Inorg. Chem.* **2008**, 47, 1925.
- (35) Langley, S. K.; Chilton, N. F.; Massi, M.; Moubaraki, B.; Berry, K. J.; Murray, K. S. *Dalton Trans.* **2010**, 39, 7236.
- (36) Riahi, A.; Wurster, M.; Lalk, M.; Lindequist, U.; Langer, P. *Bioorg. Med. Chem.* **2009**, 17, 4323.
- (37) Gilli, P.; Pretto, L.; Bertolasi, V.; Gilli, G. *Acc. Chem. Res.* **2009**, 42, 33.
- (38) Steiner, T. *Angew. Chem.* **2002**, 114, 50.
- (39) Bunting, J. W.; Kanter, J. P.; Nelander, R.; Wu, Z. N. *Can. J. Chem.* **1995**, 73, 1305.
- (40) Addison, A. W.; Rao, T. N.; Reedijk, J.; van Rijn, J.; Verschoor, G. C. *Dalton Trans.* **1984**, 1349.
- (41) Clegg, J. K.; Lindoy, L. F.; Moubaraki, B.; Murray, K. S.; McMurry, J. C. *Dalton Trans.* **2004**, 2417.
- (42) Clegg, J. K.; Lindoy, L. F.; McMurry, J. C.; Schilter, D. *Dalton Trans.* **2006**, 3114.
- (43) Hori, A.; Arii, T. *CrystEngComm* **2007**, 9, 215.
- (44) Michalska, D.; Hernik, K.; Wysokiński, R.; Morzyk-Ociepa, B.; Pietraszko, A. *Polyhedron* **2007**, 26, 4303.
- (45) Choudhury, S. R.; Lee, H. M.; Hsiao, T.-H.; Colacio, E.; Jana, A. D.; Mukhopadhyay, S. *J. Mol. Struct.* **2010**, 967, 131.
- (46) Dong, W.-K.; Sun, Y.-X.; He, X.-N.; Tong, J.-F.; Wu, J.-C. *Spectrochim. Acta, Part A* **2010**, 76, 476.
- (47) Helios, K.; Wysokiński, R.; Zierkiewicz, W.; Proniewicz, L. M.; Michalska, D. *J. Phys. Chem. B* **2009**, 113, 8158.
- (48) Castineiras, A.; Sicilia-Zafra, A. G.; González-Pérez, J. M.; Choquesillo-Lazarte, D.; Niclós-Gutiérrez, J. *Inorg. Chem.* **2002**, 41, 6956.
- (49) Wells, A. F. *Three-Dimensional Nets and Polyhedra*; Wiley-Interscience: New York, 1977.
- (50) Fages, F. *Angew. Chem.* **2006**, 118, 1710.
- (51) Hirst, A. R.; Escuder, B.; Miravet, J. F.; Smith, D. K. *Angew. Chem.* **2008**, 120, 8122.
- (52) Maeda, H. *Chem.—Eur. J.* **2008**, 14, 11274.
- (53) Piepenbrock, M.-O. M.; Lloyd, G. O.; Clarke, N.; Steed, J. W. *Chem. Rev.* **2010**, 110, 1960.
- (54) Piepenbrock, M.-O. M.; Clarke, N.; Steed, J. W. *Soft Matter* **2010**, 6, 3541.
- (55) Terech, P.; Chachati, C.; Gaillard, J.; Giroudgodquin, A. M. *J. Phys. (Paris)* **1987**, 48, 663.
- (56) Hanabusa, K.; Maesaka, Y.; Suzuki, M.; Kimura, M.; Shirai, H. *Chem. Lett.* **2000**, 1168.
- (57) Foster, J. A.; Steed, J. W. *Angew. Chem., Int. Ed.* **2010**, 49, 2.